Chapter 4 Simulation (2) – Surface Corrugation

After optimizing the C-aperture dimensions, the simulations pursued to the second stage – applying and optimizing the surface corrugation in order to draw supports from the surface plasmon excitation and to achieve a further transmission enhancement and spot size reduction. This concept will be rudimentarily analyzed in the freestanding case.

4.1 Simulation Description

4.1.1 Optical Model

The optical model is basically the same as that in Fig. 3.1-1(a) except a groove encircling the aperture.

4.1.2 Parameters

The C-aperture in this chapter is the optimum one of the freestanding case derived in chapter 3, and the protagonist here is a groove. The configurations of the C-aperture and the groove are depicted in Fig. 4.1-1.
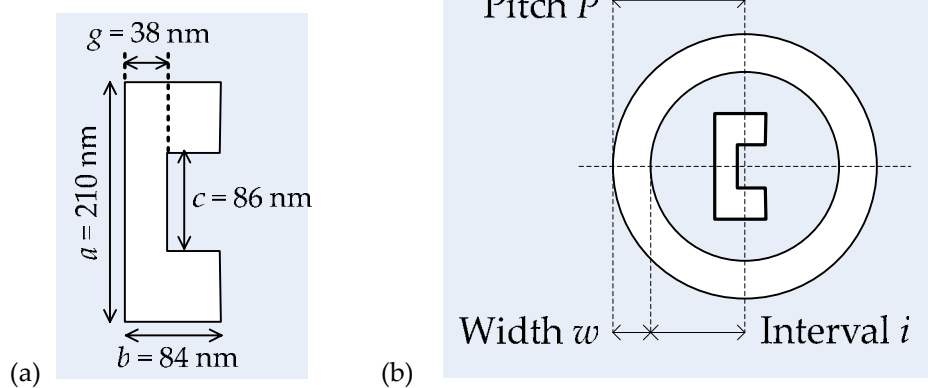

Fig. 4.1-1 (a) The C-aperture dimension (b) parameters of the groove

4.1.3 Evaluation Factors

In addition to the power throughput (PT) and the power throughput density (PTD), coupling efficiency (CE) is introduced to quantify the extent of power

throughput enhancement due to the surface plasmon polariton coupling to the photons. Therefore, its definition is:

$$CE = \frac{PT \text{ of the aperture with a groove}}{PT \text{ of the aperture without a groove}}$$

4.2 Results (1) – Incident-side Groove

4.2.1 Rectangular Aperture

The previous investigations all focused on a circular aperture surrounded by grooves, here the attention was riveted on a rectangular aperture encircled by a groove at incident face to clarify the effects of the aperture shape on SPP excitation and coupling. Since surface plasmons are easily excited by the incident photons with wavelength approximated to the groove pitch, a groove of pitch P 600 nm is applied to surround the rectangular aperture. Besides, the groove width w and groove interval i are 240 nm and 360 nm respectively, as illustrated in Fig. 4.2-1, which is the same as Ebbesen's simulation [1] so that the results can be easily compared.
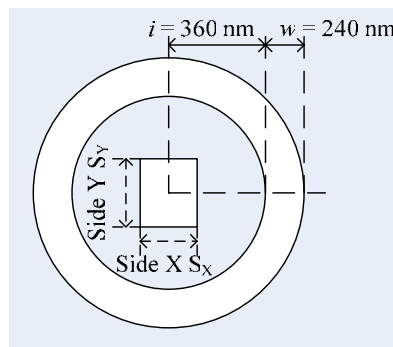

Fig. 4.2-1 Configurations of a rectangular aperture with a groove

According to Fig. 4.2-2, the power throughput of a rectangular aperture is still enhanced, suggesting the aperture shape is a minor issue of SPP excitation. The coupling efficiency, as listed in Table 4.2-1, indicates the coupling effect grows stronger with the decreasing aperture size. This phenomenon may be ascribable to that the photons confined in a narrower aperture possess higher momentum so that they are capable of exciting the surface plasmons more effectively and the probability of the coupling effect is increased accordingly.

Compared to the coupling efficiency of a circular aperture in Ebbesen's results, around 5, the rectangular aperture with such a groove performs competently in this

simulation. Therefore, a further transmission enhancement is probably achieved with the C-aperture with a groove by optimizing the groove.
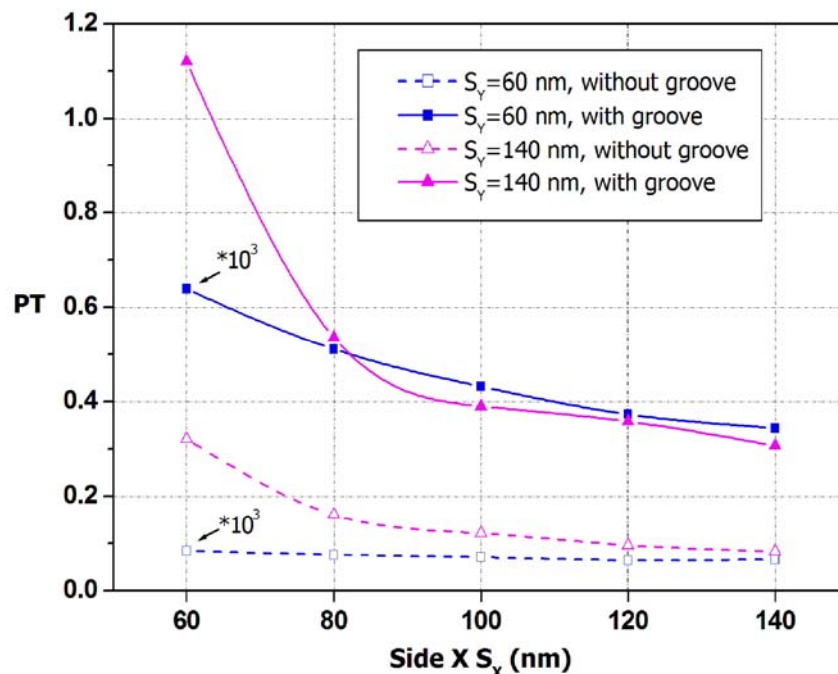

Fig. 4.2-2 Power throughput of various rectangular apertures, and while S_Y=60 nm, the power throughput is magnified by three orders.

Table 4.2-1 Coupling efficiency of various rectangular apertures

S_Y = 60 nm				
S_X (nm)	60	80	100	120	140
CE	7.61	6.72	6.13	5.79	5.17
S_Y = 140 nm				
S_X (nm)	60	80	100	120	140
CE	3.49	3.32	3.23	3.74	3.70

4.2.2 C-shaped aperture

The aim of this section is to arrive at a further transmission enhancement via an incident-side groove encircling the C-aperture. The C-aperture is the optimum one derived in chapter 3 and the parameters of the incident-side groove are schematically plotted in Fig. 4.2-3.
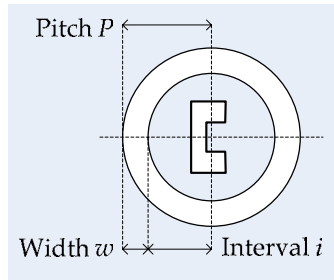
Fig. 4.2-3 Parameters of an incident-side-corrugated C-aperture

Generally, the power throughput of this incident-side-corrugated C-aperture, as shown in Fig. 4.2-4, is higher than that of a single optimum C-aperture, which is 1.77, indicating the excited SPPs are antisymmetric modes that possess sufficient propagation length to enhance the field. The differences among each line shape can be explained by quantum mechanics [2], which treats a groove as an energy well. Since the width of the energy well determines how many and which quantum modes exist, different groove width will produce different sets of SPP antisymmetric eigenmodes, which are responsible for dissimilar tendency of the power throughput in Fig. 4.2-4.

Since the emitted SPP mode is superposed by several SPP eigenmodes as

Emitted SPP mode = $a_1 (SPP_1) + a_2 (SPP_2) + a_3 (SPP_3) + ...$
SPP_x, $x = 1, 2, ...$are the anti-symmetric SPP eigenmodes with fixed groove width,
a_x, $x = 1, 2, ...$are the weighting factors of the SPP_x mode

the different interval i with a fixed groove width w leads to different the weighting factors; on the other word, the superposed SPP field distribution is changed with different interval i. Since each SPP eigenmode carries different momentum and energy, a variation in the power throughput of each curve in Fig. 4.2-4 is reasonable to take place. The higher power throughput implies a more well-matched momentum and energy conservation conditions; as a result, the SPPs can couple to the incident photons more effectively and result in a stronger transmission enhancement.
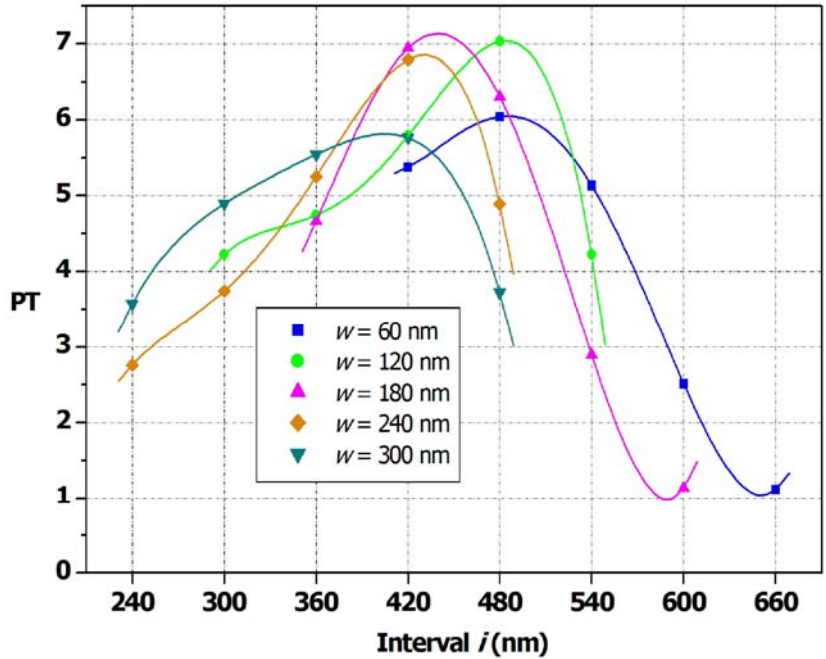
Fig. 4.2-4 Power throughput of incident-side-corrugated C-apertures as functions of interval *i* and width *w*

    The role of the groove pitch *P* plays may be revealed in Fig. 4.2-5, where each power throughput with a fixed interval *i* undulates gradually with a peak at pitch of 620 nm. The groove pitch *P* is a provision of the lattice momentum [3] which is auxiliary to fulfill the momentum conservation during the interaction between the photons and the surface plasmons; therefore, groove pitch involves with the probability of the coupling between photons and surface plasmons, slightly affecting the power throughput enhancements accordingly.

    Since silver is a transition metal so that its electron distributions are considerably complicated, an exact mathematical expression of the interaction among the electron, photon and surface plasmon is formidably difficult to derive; however, employing the fundamental physical science, the effects of each groove parameter are clarified and grasped in this work.
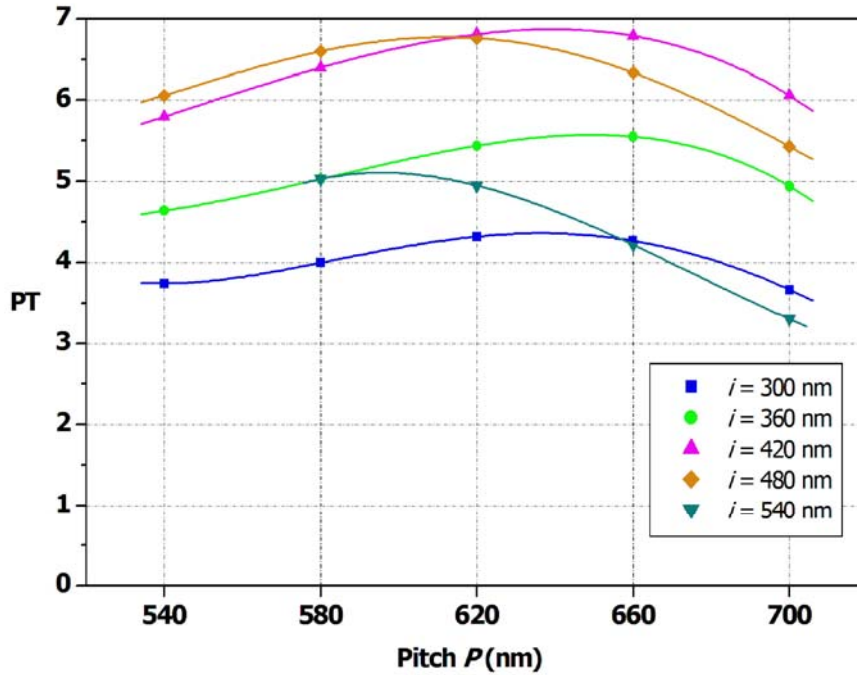
Fig. 4.2-5 Power throughput of incident-side-corrugated C-apertures as functions of interval i and pitch P

The coupling efficiency is calculated by dividing each power throughput in Fig. 4.2-4 by 1.77, which is the power throughput of the single C-aperture without a groove, and the maximum value is ~3.88. That the CE is not as high as that of the rectangular aperture cases in section 4.2.1 is attributable to the funnel effect taking place in front of the C-aperture, which changes the momentum of the photons and then hampers the coupling effect; nevertheless, such an incident-side groove can still contribute to a further enhancement in power throughput. Besides, the simulation results also show that the spot size is rarely affected, and hence, the improvements in optical performance primarily hinge on the power throughput enhancement.

The optical performances of a single $60*60 \text{ nm}^2$ square aperture, the optimum single C-aperture and the optimum incident-side-corrugated C-aperture are particularized in Table 4.2-2 with their configurations plotted in Fig. 4.2-6. Compared to the single C-aperture and a $60*60 \text{ nm}^2$ square aperture, the power throughput of the incident-side-corrugated C-aperture is enhanced by a factor of 3.88 and 10^5 respectively at a spot size identical to that of the single C-aperture.

Table 4.2-2 Comparison of the 60*60 nm² square aperture, the optimum C-aperture and the optimum incident-side-corrugated C-aperture

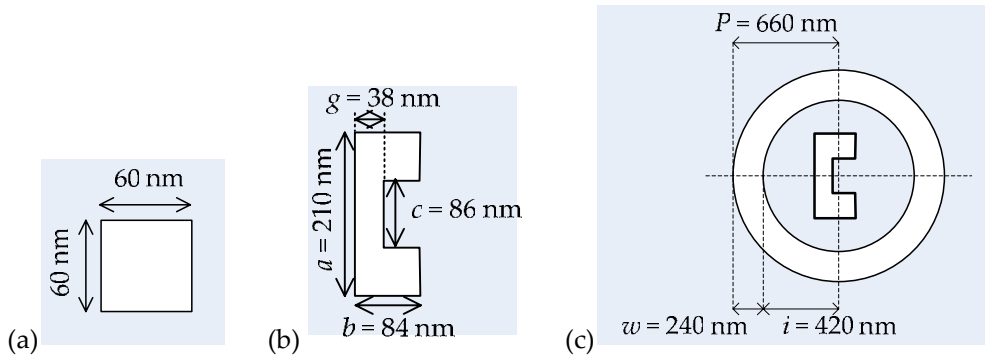| Aperture type	Square	C-shaped	Incident-side-corrugated C-shaped
Power throughput	6.42E-05	1.77E+00	6.79E+00
Spot size (nm*nm)	147*111	117.8*136.4	117.8*136.4
Power throughput density	3.93E-03	1.10E+02	4.04E+02

Fig. 4.2-6 Configurations of (a) square aperture, (b) optimum C-aperture and (c) optimum incident-side-corrugated C-aperture

4.3 Exit-side Groove

Going a step further, another groove is applied on the exit face for further improvements in the optical performance. The film of 200 nm is thick (more than 5 times skin depth of 25 nm) enough to manipulate SPP modes on the opposite sides independently; therefore, the incident-side groove is adopted as the optimized one derived in section 4.2. The aperture configurations at both the incident and exit faces are depicted in Fig. 4.3-1
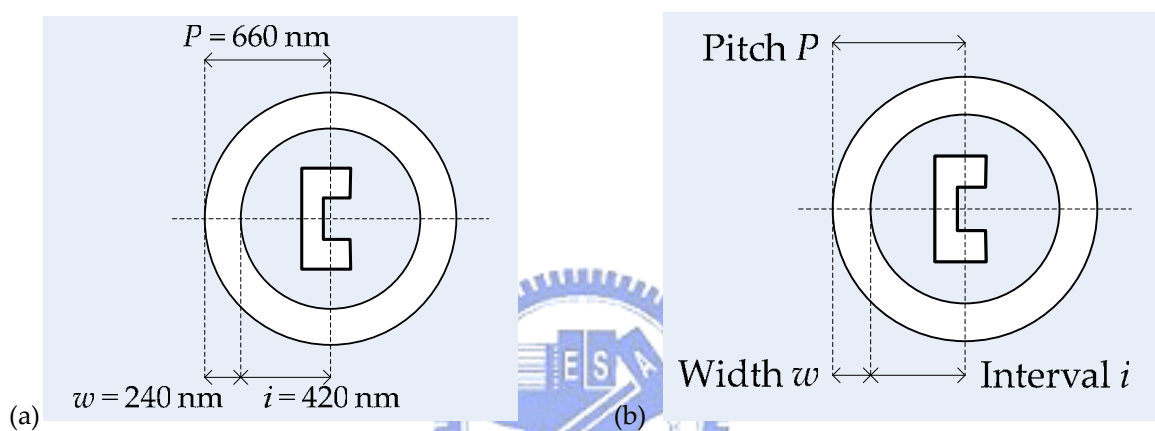

Fig. 4.3-1 Configuration of a double-side-corrugated C-aperture at (a) incident and (b) exit face

Based on the surface plasmon theory, the exit-side groove is conductive to SPP excitation as well; however, the thick film will prevent the incident photons from penetrating and interacting with the electrons at the exit face. Under this circumstance, the incident SPP modes that can propagate across the film are primarily responsible for the excitation of the exit SPP modes, and then, they will interfere with each other. Naturally, these "SPP-driven" SPP modes will carry weaker energy than those "photon-driven" ones at incident face; thereupon, the power throughput of the double-side-corrugated C-aperture, ~8, is only a little stronger than the highest one of the incident-side-corrugated C-aperture, ~6.79.

Although the power throughput is not increased much, there is still a noteworthy matter resting on the regular behavior of the power throughput as a function of interval i. Since the interaction between the SPP modes on opposite faces

is in an interference style, the peaks shown in Fig. 4.3-2 can be considered as a constructive interference while the sharp decline reveals a destructive superposition of their individual field distributions. This result is consistent with the inference that the interval i is the critical factor to the field distribution.
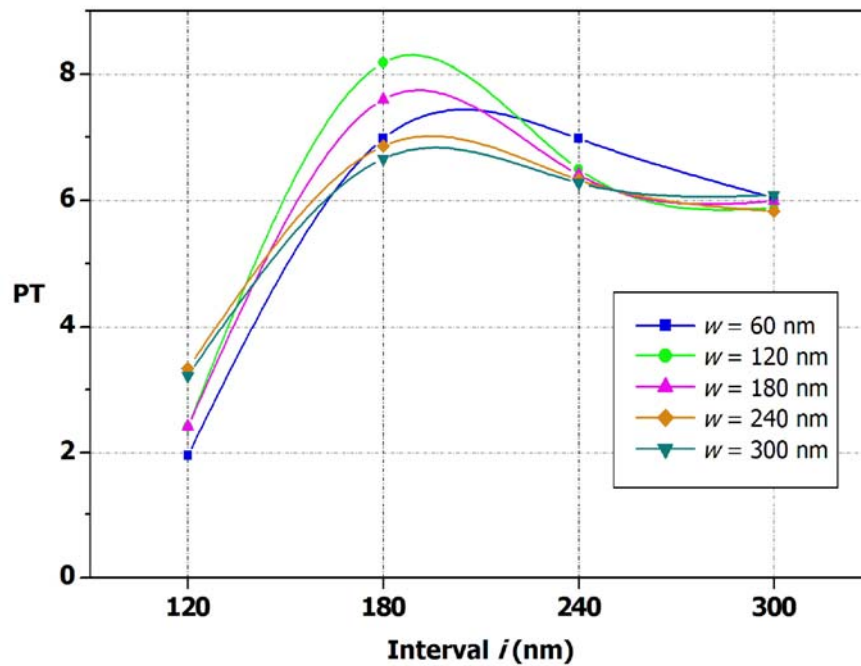

Fig. 4.3-2 Power throughput of the double-side-corrugated C-apertures as a function of interval i

The emitted optical profile of the double-side-corrugated C-aperture will differ from that of the incident-side-corrugated one owing to the interference, and the change in the superposed field distribution will be reflected by the variation of the spot size. As a result of the X-polarized incident light, the spot size in X-direction is greatly altered; in contrast, it only slightly varies in Y-direction, as listed in Table 4.3-1. Inasmuch as the SPPs are highly associated with the electric field of the incident light, the attention is drawn on the spot size in X-direction, which is diagrammed in Fig. 4.3-3. Apparently, the exit groove functions as a focusing grating at interval i of 240 nm, signifying that the field distribution of this exit SPP mode will cause a more convergent optical profile of the emitted light. Besides, the more dramatic variation with a narrower groove width can be explained again by

quantum mechanics, which states that the particle confined in a narrower potential well will oscillates more strongly, resulting in a greater alternation in field distribution of the emitted light.

Table 4.3-1 Spot size in (a) X-direction and (b) Y-direction

width w (nm) / interval i (nm)	60	120	180	240	300
120	182.4	201.4	201.4	167.2	133.0
180	186.2	159.6	129.2	102.6	114.0
240	110.2	106.4	102.6	106.4	114.0
300	142.6	142.6	106.4	110.2	114.0

(a)

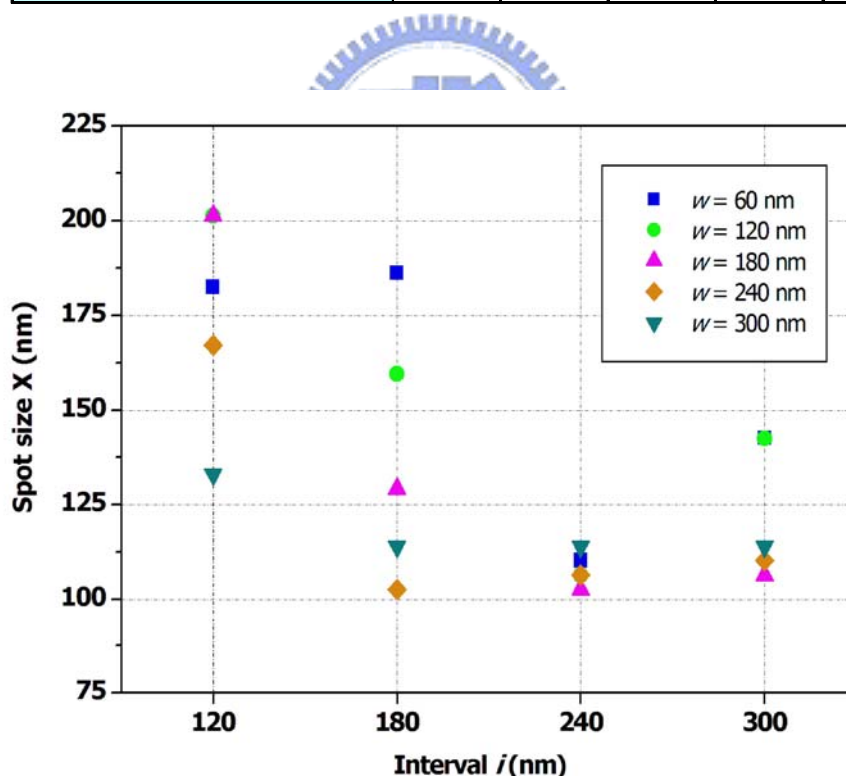| width w (nm) / interval i (nm)	60	120	180	240	300
120	148.8	155.0	155.0	155.0	148.8
180	142.6	142.6	142.6	130.2	142.6
240	142.6	142.6	130.2	130.2	142.6
300	142.6	142.6	130.2	130.2	142.6

(b)

Fig. 4.3-3 Spot size of the double-side-corrugated in X-direction as a function of interval i

According to the aforementioned results, the maximum power throughput and the minimum spot size correspond to different parameters of the exit-side groove; hence, the optical performance should be evaluated by power throughput density,

which makes a compromise between the power throughput and the spot size. As shown in Fig. 4.3-4, the highest power throughput density occurs at interval i of 180 nm and width w of 240 nm, where the power throughput is 6.86 at the spot size of 102.6*130.2 nm². Compared to the incident-side-corrugated C-aperture, although the power throughput is only enhanced little, the spot size is much reduced by 30%
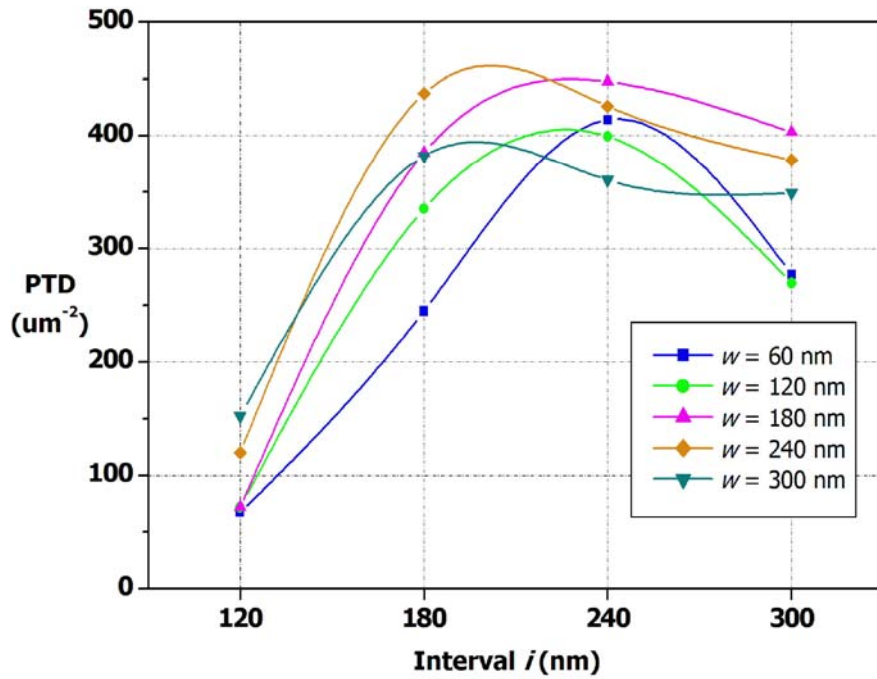

Fig. 4.3-4 Power throughput density of the double-side-corrugated C-apertures

4.4 Summary

While an incident-side groove is introduced, manipulating its interval and width that determine which SPP mode is excited and how the field distributes will raise the power throughput by the coupling effect between incident photons and SPPs. On the other hand, once an exit-side groove is applied as well, the exit SPP modes will superpose to the incident ones, which subsequently causes a variation in the optical profile of the emitted light and has a great impact on the spot size.

In order to show the evolution of the aperture designs and the improvements in each phase, their configurations and optical performances are illustrated and listed in Fig. 4.4-1 and Table 4.4-1 respectively. The great advance of power throughput, which is enhanced by a factor of $2.76*10^4$, is attributed to the funnel effect and the propagation mode of the C-aperture; in addition, the incident-side groove also enhance the power throughput by a factor of 3.84. The spot size reduction of 30% is ascribable to the exit-side groove which acts as a focusing grating. Eventually, the double-side-corrugated C-aperture renders a factor of $1.31*10^5$ increase in power throughput density in comparison with a $60*60$ nm^2 square aperture.

Table 4.4-1 Comparison of the square, optimum C-aperture, optimum incident-side-corrugated
C-aperture and double-side-corrugated C-aperture

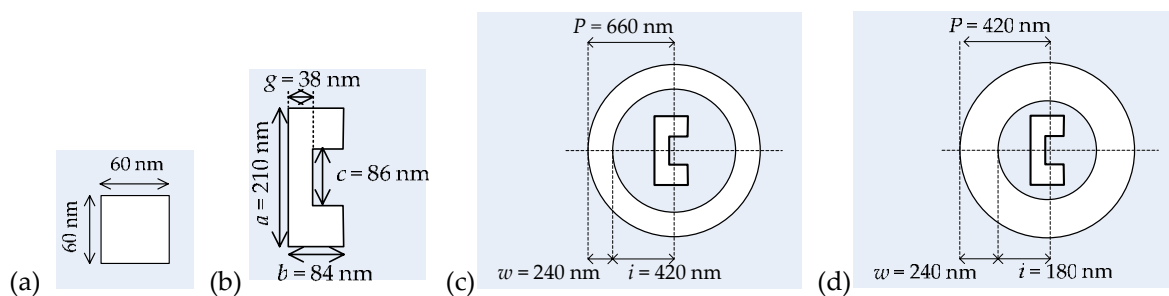| Aperture type	Square	C-shaped		
		Single	incident groove	incident & exit grooves
Power throughput	6.42E-05	1.77E+00	6.79E+00	6.86E+00
Spot size (nm*nm)	147*111	117.8*136.4	117.8*136.4	102.6*130.2
Power throughput density	3.93E-03	1.10E+02	4.04E+02	5.13E+02

Fig. 4.4-1 Configurations of (a) square aperture, (b) optimum C-aperture, (c) single-corrugated C-aperture and (d) the exit face of the double-corrugated C-aperture with incident-side groove as (c)